

Article

# Low Temperature Raman Spectroscopy of Tetrahydrofuran: Phonon Spectra Compared to Matrix Isolation Spectra in Air

Vlasta Mohaček-Grošev 

Center of Excellence for Advanced Materials and Sensing Devices, Research Unit New Functional Materials, Ruđer Bošković Institute, Bijenička cesta 54, 10000 Zagreb, Croatia; mohacek@irb.hr

**Abstract:** The conformation of tetrahydrofuran (THF) molecules in vapor has been the subject of considerable computational and experimental studies, the most recent by Park and Kwon stated that the difference between the most stable, twisted  $C_2$  conformer and the bent  $C_s$  conformer is  $17 \pm 15 \text{ cm}^{-1}$ . Because of low symmetry, all modes from both conformers are allowed in the Raman and infrared spectra. In 1982, Aleksanyan and Antipov observed the emergence of two Raman bands at 249 and  $303 \text{ cm}^{-1}$  at 20 K, while only one band at  $293 \text{ cm}^{-1}$  was present in solid THF at 142. They assigned the  $249 \text{ cm}^{-1}$  band to the restricted pseudorotational motion of THF in the solid state, because on heating, the band diminishes and is too weak to be observed near melting point (at 142 K). Cadioli et al. reported a study of the vibrational spectrum of tetrahydrofuran, giving a complete assignment of all bands including those present in the low-temperature Raman spectrum at 85 K and infrared bands observed at 90 K. They assigned the band at  $242 \text{ cm}^{-1}$  in the Raman spectrum at 85 K as an overtone of the lowest normal mode (pseudorotational mode), while the  $299 \text{ cm}^{-1}$  band in the same spectrum was assigned as a radial mode. In the following, low-temperature Raman spectra of solid THF together with the Raman matrix isolated spectrum of THF in air will be presented and compared to published data. Our results indicate that the band observed at  $245 \text{ cm}^{-1}$  at 10 K is too strong to be assigned as an overtone, since its intensity is of the same magnitude as the  $299 \text{ cm}^{-1}$  band.

**Keywords:** tetrahydrofuran; Raman; matrix isolation; crystal; low temperature; pseudorotation; ring puckering



**Citation:** Mohaček-Grošev, V. Low Temperature Raman Spectroscopy of Tetrahydrofuran: Phonon Spectra Compared to Matrix Isolation Spectra in Air. *Crystals* **2024**, *14*, 468. <https://doi.org/10.3390/cryst14050468>

Academic Editor: Luis M. Garcia-Raffi

Received: 22 April 2024

Revised: 9 May 2024

Accepted: 14 May 2024

Published: 16 May 2024



**Copyright:** © 2024 by the author. Licensee MDPI, Basel, Switzerland. This article is an open access article distributed under the terms and conditions of the Creative Commons Attribution (CC BY) license (<https://creativecommons.org/licenses/by/4.0/>).

## 1. Introduction

The non-rigidity of small molecules has captured the interest of scientists because it is essential for explaining their chemical preferences, such as conformations of amino acids in peptides [1], for the determination of the composition of sugars in solutions [2], and for explaining the origin of modern twist–bend nematic liquid crystals [3], among others. As pointed out by Park and Kwon, structural variations of ribose having  $C_{2'}$ -endo conformation in B-deoxyribonucleic acid and  $C_{3'}$ -endo conformation in ribonucleic acid have an impact on their biological function [4]. Tetrahydrofuran is produced and used in large quantities reaching nearly half a million tons per year [5], because it can solvate both polar and non-polar compounds [6] and is a candidate for hydrogen storage due to its ability to form clathrate hydrates [7].

The conformation of tetrahydrofuran (THF) molecules in vapor has been the subject of considerable computational and experimental studies [8–11], the most recent of which stated that the difference between the most stable twisted  $C_2$  conformer and the bent  $C_s$  conformer is  $17 \pm 15 \text{ cm}^{-1}$  [4]. Because of low symmetry, all modes are allowed in both the Raman and the infrared spectrum. However, the transitions between pseudorotational levels for THF in the gas phase require special attention, since the two lowest normal modes, pseudorotational and radial transition, display a multitude of sub-transitions [12–16].

In the solid state, it has been repeatedly established by both X-ray [5,17] and neutron scattering [18] that THF exists in the twisted  $C_2$  conformation. It crystallizes in the  $C2/c$  space group with four molecules per unit cell, each molecule being on the rotation axis of symmetry of the second order [17]. Aleksanyan and Antipov observed the emergence of two Raman bands at 249 and 303  $\text{cm}^{-1}$  at 20 K, while only one band at 293  $\text{cm}^{-1}$  was present in solid THF at 142 K [19]. They assigned the two bands to the out-of-plane skeletal vibrations of THF in restricted non-planar conformation. Cadioli et al. reported a study on the vibrational spectrum of tetrahydrofuran, giving a complete assignment of all bands including those present in low-temperature Raman spectrum at 85 K and infrared bands observed at 90 K [20]. They assigned the band at 242  $\text{cm}^{-1}$  in the Raman spectrum at 85 K as an overtone of  $\nu_{33}$ , which is the lowest normal mode (pseudorotational mode), while the 299  $\text{cm}^{-1}$  band in the same spectrum was assigned as a radial mode ( $\nu_{17}$ ). In a subsequent publication, Gallinella et al. presented vibrational spectra THF- $d_8$ , assigning the two Raman bands observed in the solid at 125 and 199  $\text{cm}^{-1}$  to  $0 \rightarrow 1$  and  $0 \rightarrow 2$  jumps of the pseudorotational motion [21].

Recently, an FTIR matrix isolation experiment was conducted where THF molecules were immobilized in  $\text{N}_2$ , and the conclusion based on repeated annealing was that both  $C_s$  and  $C_2$  were present in the matrix independently of the annealing process [22]. Also, Park and Kwon used mass spectroscopy combined with vacuum UV photoionization to produce a THF cation in the  $D_0$  state, which was predominantly in the  $C_2$  conformation, and analyzed data for both  $C_2$  and  $C_s$  conformations in the ground  $S_0$  state of the neutral molecule [4]. They determined the conformational stabilities of the twisted  $C_2$  and bent  $C_s$  conformers to be  $17 \pm 15 \text{ cm}^{-1}$ , and stated that they can equilibrate under the molecular beam conditions applied in the experiment [4].

In the following, low-temperature Raman spectra of solid THF together with the Raman matrix isolated spectrum of THF in air will be presented and compared to published data. To the best of the authors' knowledge, no previous Raman matrix isolation spectra of tetrahydrofuran have been published so far. Our results indicate that the band observed at 245  $\text{cm}^{-1}$  at 10 K is too strong to be assigned as an overtone, as was assigned in [20].

## 2. Experimental

Liquid tetrahydrofuran was purchased from VWR company; it had a purity > 99% and was used as such. The experimental setup for Raman matrix isolation experiments has been described previously [23,24]; therefore, we briefly stress the main points. A closed-cycle helium cryostat is used for the cooling of the cold finger in the sample chamber onto which a gold-plated surface is fixed. Once the lowest attainable temperature is achieved (10 K), the valve that lets the mixture of air and tetrahydrofuran vapor is opened. Within several minutes, a solid film of frozen air and THF molecules is formed on the gold-plated surface, and Raman spectral acquisition undertaken. Since the vapor pressure of tetrahydrofuran is 18.8 kbar at 295 K [25], at atmospheric pressure of 101,325 Pa, there are 5.4 molecules of nitrogen or oxygen per one molecule of tetrahydrofuran present. Their vibrations, however, are not overlapping vibrational bands of tetrahydrofuran, since they are observed at 2328  $\text{cm}^{-1}$  ( $\text{N}_2$ ) and at 1553  $\text{cm}^{-1}$  ( $\text{O}_2$ ). For cooling, we used a CCS 350 Janis Research closed cycle He cryostat with Lake Shore 331 temperature controller. Spectra were recorded with a T64000 Horiba-JobinYvon Raman spectrometer, operating in triple subtractive mode. Raman spectra were recorded in multiwindow option, from 10 to 3200  $\text{cm}^{-1}$  for the polycrystalline sample and from 50 to 3200  $\text{cm}^{-1}$  for the liquid and matrix isolated THF. The laser power of the 532 nm DPSS laser (ChangChun Industries Ltd., Changchun, China) applied to the sample was 7 mW. Pure THF spectra of polycrystalline THF were obtained after a small amount of sample was sealed in a glass tube and mounted in the sample chamber of the cryostat. In Figure 1, an overview of Raman spectra of THF in liquid (295 K, 150 K) and crystal phases (120 K, 10 K) is given. In Figure 2, the high wavenumber regions (2400–3100  $\text{cm}^{-1}$ ) of the spectra are compared for matrix isolated, liquid and crystalline THF, while the middle parts of the same spectra are shown in Figures 3 and 4.

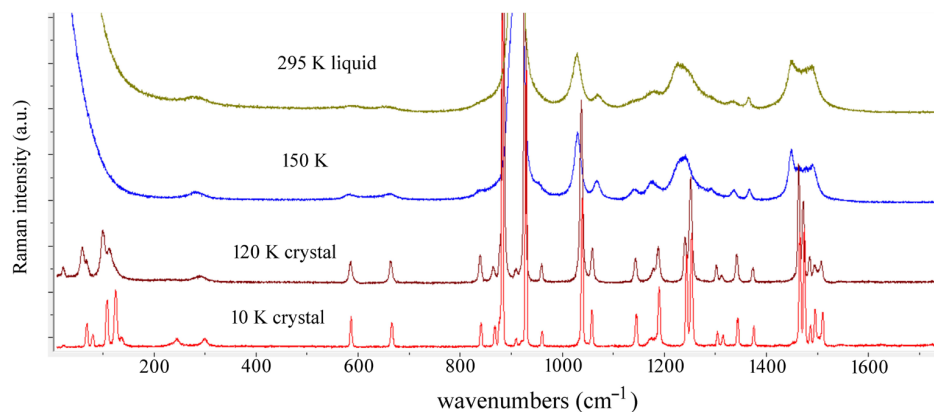


**Figure 1.** Raman spectra of THF in liquid (295 K, 150 K) and crystal phases (120 K, 10 K) from 10 to 1600  $\text{cm}^{-1}$  (solid) and 50 to 1600  $\text{cm}^{-1}$  (liquid). The spectra of liquids do not show the top of the very strong band at 914  $\text{cm}^{-1}$  in order to provide a better view of weaker bands (see Figure 4).

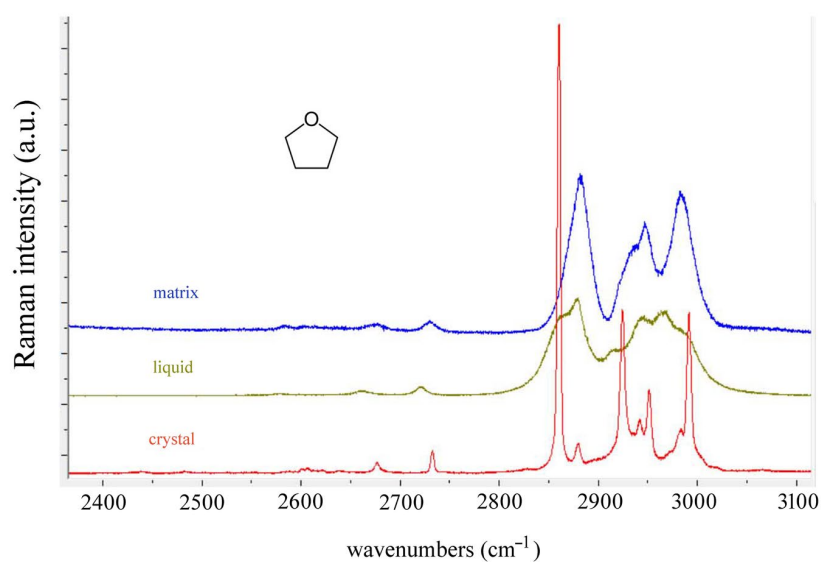


**Figure 2.** Raman spectra of THF in matrix (10 K), liquid (295 K) and crystal phases (10 K) from 2400 to 3100  $\text{cm}^{-1}$ .

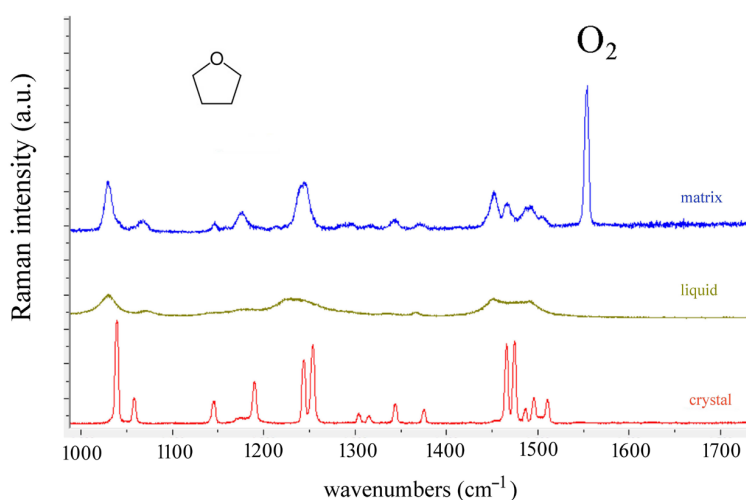


**Figure 3.** Raman spectra of THF in matrix (10 K), liquid (295 K) and crystal phases (10 K) from 1000 to 1700  $\text{cm}^{-1}$ .

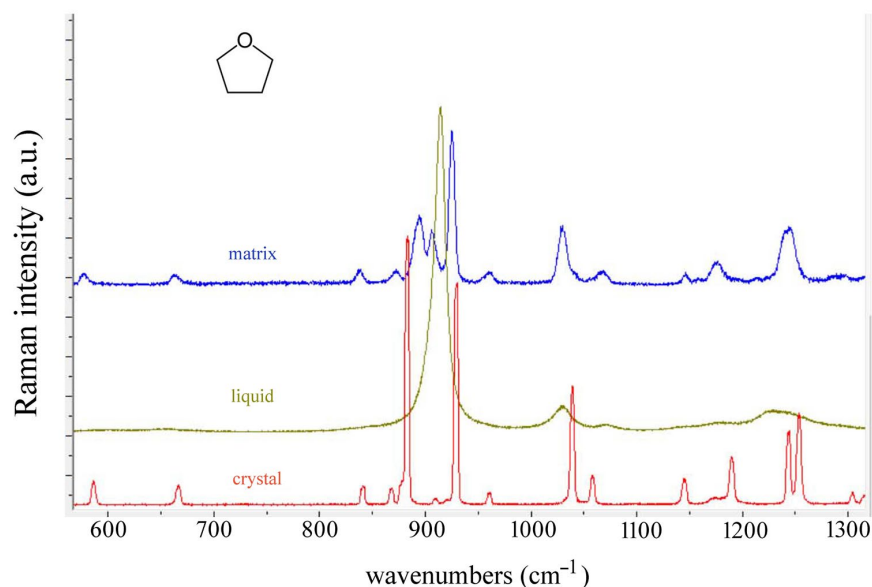


**Figure 4.** Raman spectra of THF in matrix (10 K), liquid (295 K) and crystal phases (10 K) from 580 to 1300  $\text{cm}^{-1}$ .

### 3. Computational Details

Normal modes of tetrahydrofuran in  $C_2$  and  $C_s$  conformation (Figure 5) were calculated using Gaussian09 [26] at the b3lyp/6-31++G(d,p) level of theory. All frequencies turned out positive. The difference in the ground state energies of the two conformers was only  $5.7 \cdot 10^{-5}$  Ha, or 0.46 meV. The  $C_2$  conformer was found to have lower energy.

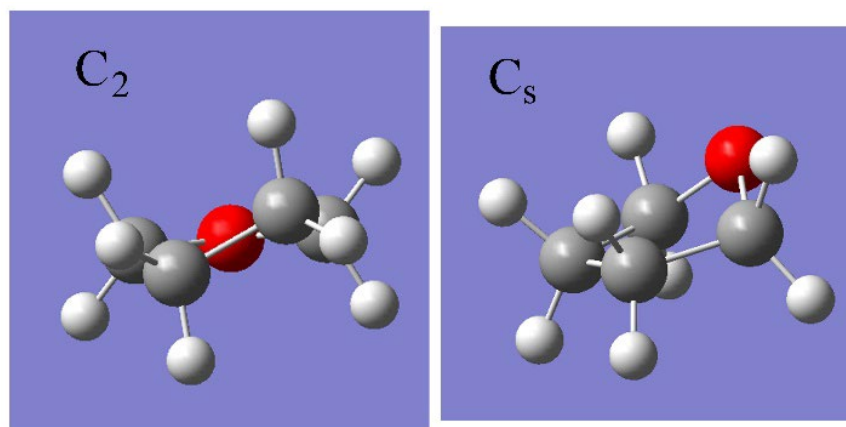


**Figure 5.** Optimized geometrical structures of the most stable  $C_2$  conformer and the  $C_s$  conformer. Oxygen atom is shown in red.

### 4. Results and Discussion

Comparing the Raman spectra of matrix isolated THF with those of liquid (Figures 2–4 and Figure 6), one observes the better resolving of vibrational transitions, especially in the 1100–1500  $\text{cm}^{-1}$  interval (Figure 3). Four normal modes have their corresponding transitions at 1492, 1487, 1466, and 1452  $\text{cm}^{-1}$ , while the 1506  $\text{cm}^{-1}$  band was assigned as the combination  $\nu_{15} + \nu_{16}$  (Table 1). Whereas in the liquid, a few broad bands can be identified between 1100 and 1300  $\text{cm}^{-1}$ , in the matrix one observes bands at 1371, 1343, 1317, and 1296  $\text{cm}^{-1}$ , which are assigned as  $\nu_7$ ,  $\nu_{24}$ ,  $\nu_8$ , and  $\nu_{25}$  of the twisted conformer,  $C_2$ . The band at 1287  $\text{cm}^{-1}$  is assigned as  $\nu_{25}$  of the THF molecule at the second matrix site. Bands at 1179, 1227 and 1253  $\text{cm}^{-1}$  observed in Raman spectrum of liquid have their counterparts in 1176, 1239 and 1246  $\text{cm}^{-1}$  bands observed for matrix isolated THF

(Figure 3). The strongest band in liquid is observed at  $914\text{ cm}^{-1}$ , while in the matrix isolated THF there are bands at  $872$ ,  $894$ ,  $906$ ,  $925$ , and  $961\text{ cm}^{-1}$  (Figure 4, Table 1). Stocka et al. assigned the bands at  $1013.9$  and  $1079.1\text{ cm}^{-1}$  to  $C_s$  conformers, and these bands had their intensity diminished after annealing [22]. We observed a weak band at  $1066\text{ cm}^{-1}$  and assigned it to  $\nu_{28}$  of the  $C_2$  conformer.

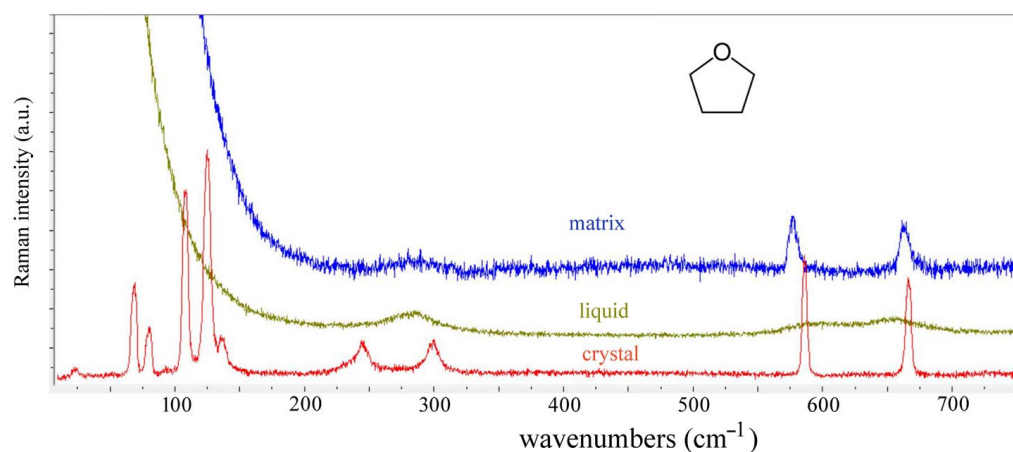


**Figure 6.** Raman spectra of THF in matrix (10 K) and liquid (295 K) from  $50$  to  $700\text{ cm}^{-1}$  compared to Raman spectrum of polycrystalline THF at  $10\text{ K}$  from  $10$  to  $700\text{ cm}^{-1}$ .

**Table 1.** Observed bands in Raman spectra of tetrahydrofuran in matrix (10 K), crystal (10 K) and liquid (295 K). The assignment of fundamentals is taken from Cadioli et al. [20].

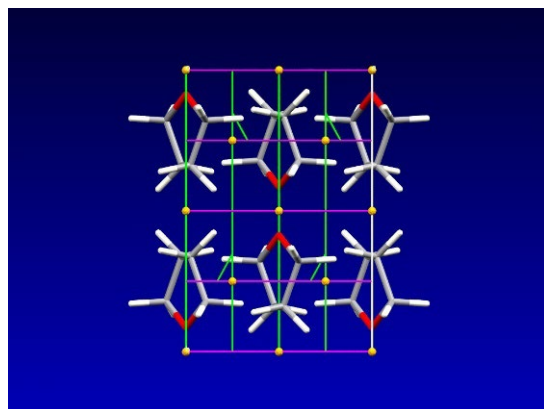
Observed Bands in Raman Spectra of Tetrahydrofuran				
Matrix Isolated 10 K	Assignment $C_2$ Conformer	Crystal 10 K $C_2$ Conformer	Liquid 295 K	Assignment from [20]
		3019 w		
		3003 mw, sh		
		2992 s	2988 s, sh, br	$2\nu_5$
2984 s, br	$\nu_1$	2983 m		
		2972 mw, sh		
			2964 s, br	$\nu_1$
2947 s, br	$\nu_2$	2951 ms		
		2943 m	2943 s, br	$\nu_2$
2935 ms, br	$\nu_3$	2935 m, sh		
		2924 ms, sh		
			2915 s, br	$\nu_3$
2881 s, br	$\nu_4$	2880 m	2878 s	$\nu_4$
		2860 vvs	2864 s, sh	
2729 w	$\nu_{22} + \nu_{26}$	2732 m	2721 mw	$\nu_{22} + \nu_{26}$
2676 w	$\nu_5 + \nu_{10}$	2676 w	2661 w	$\nu_5 + \nu_{10}$
2328 vs. $N_2$				
1553 s, $O_2$				
1506 mw	$\nu_{15} + \nu_{16}$	1511 m		
1492 m	$\nu_5$	1496 m		
1487 m, sh	$\nu_{22}$	1487 w	1489 m, br	$\nu_5$

Table 1. Cont.

Observed Bands in Raman Spectra of Tetrahydrofuran				
Matrix Isolated 10 K	Assignment C <sub>2</sub> Conformer	Crystal 10 K C <sub>2</sub> Conformer	Liquid 295 K	Assignment from [20]
		1474 ms	1475 m, br, sh	$\nu_{22}$
1466 m	$\nu_6$	1466 ms		
1452 m	$\nu_{23}$	1453 vw	1451 m, br	$\nu_{23}$
1371 w	$\nu_7$	1375 mw	1367 w	$\nu_7$
1343 w	$\nu_{24}$	1344 m	1337 w	$\nu_{24}$
1317 vw	$\nu_8$	1315 w		
1296 w	$\nu_{25}$	1304 w		
1287 w, sh	$\nu_{25}$ second site		1288 mw, vbr, sh	$\nu_{25}$
1246 m	$\nu_{26}$	1254 ms	1253 m, vbr, sh	$\nu_{26}$
1239 m, sh	$\nu_9$	1244 ms		
1214 vw	$\nu_9$ second site		1227 m	$\nu_9$
		1190 m		
		1181 w	1179 w, br	$\nu_{10}$
1176 w	$\nu_{10}$	1173 w		
1147 w	$\nu_{11}$	1145 m	1140 w, sh	$\nu_{11}$
1066 w	$\nu_{28}$	1058 m	1072 mw	$\nu_{28}$
1030 m	$\nu_{12}$	1040 s	1030 m, br	$\nu_{12}$
961 w	$\nu_{29}$	961 mw	949 w, sh	$\nu_{29}$
925 s	$\nu_{13}$	929 vs		
		920 w		
906 m	$\nu_{30}$	910 w	914 vs	$\nu_{13}$
894 m	$\nu_{14}$	883 vs	902 s, sh	$\nu_{30}$
872 w	$\nu_{31}$	878 m, sh		
		868 m		
		848 m	844 w, sh	$\nu_{15}$
838 w	$\nu_{15}$	841 m		
662 w	$\nu_{16}$	667 m	654 w, br	$\nu_{16}$
577 w	$\nu_{32}$	586 m	598 w, br	$\nu_{32}$
		299 mw, br		$\nu_{17}$ radial mode
283 vw, br	$\nu_{17}$		284 w	$\nu_{17}$ radial mode
		245 mw, asym, br		$\nu_{33}$ quasi pseudorotational mode
		136 mw		lattice mode
		125 m		lattice mode
		108 m		lattice mode
		94 w		lattice mode
		80 mw		lattice mode
		69 mw		lattice mode
		24 w		lattice mode

The bands in spectrum of polycrystalline THF are much narrower, showing splitting due to molecular packing in the unit cell. The crystal structure of tetrahydrofuran was solved by Luger and Buschmann [17]. THF crystallizes in the C<sub>2/c</sub> space group, having

$Z = 4$ , and unit cell dimensions equal to  $a = 607.6(9)$  pm,  $b = 891.4(9)$  pm,  $c = 774.3(11)$  pm and  $\beta = 106.11(12)^\circ$  (see Figure 7). Each THF molecule in the crystal lies on a  $C_2$  axes and has a  $C_2$  symmetry, with a twisted conformation. Later, David and Ibberson performed reinvestigations of the THF crystal structure using neutron scattering, and showed that the THF crystal remains stable down to 5 K [18]. Our assignment of Raman modes follows the procedure of Berenblut et al. on the  $C2/c$  structure of gypsum [27], where two molecules make a motif and  $Z = 2$ . The total number of degrees of freedom is 156, and if one removes three acoustical degrees of freedom (their symmetry is  $A_u \oplus 2B_u$ ), there are 153 vibrations left.



**Figure 7.** Crystal packing of tetrahydrofuran in the  $C2/c$  space group. Image prepared with the Mercury program [28]. Violet lines correspond to glide planes, green lines to screw axis and proper  $C_2$  axes and yellow dots to centres of inversion. Oxygen atoms are on proper  $C_2$  axes.

The resulting decomposition of the reducible representation of THF phonons without acoustic modes is

$$\Gamma_{vib} = 38 A_g \oplus 40 B_g \oplus 37 A_u \oplus 38 B_u$$

This result was derived from characters of a reducible representation, which is stated in the following. The only atoms that are placed on a symmetry element are oxygen atoms (four of them are on a proper  $C_2$  axes in a unit cell), giving the characters of the following reducible representation:  $\chi(E) = 156$ ,  $\chi(C_2) = -4$ ,  $\chi(i) = 0$ ,  $\chi(\sigma) = 0$ .

Of these modes, there are twelve vibrational and nine translational modes expected below  $250 \text{ cm}^{-1}$ . Usually called external phonons, their symmetry is found via correlation tables to be

$$\Gamma_{ext} = 4 A_g \oplus 8 B_g \oplus 3 A_u \oplus 6 B_u$$

The two lowest internal modes, restricted puckering motion and radial mode, are observed at  $245$  and  $299 \text{ cm}^{-1}$  at 10 K (Table 1, Figure 6).

Of particular interest to us is the low-frequency part of the THF Raman spectra; for the polycrystalline solid, lattice modes usually appear below  $200 \text{ cm}^{-1}$ , while in the spectra of liquid and matrix isolated THF, a Rayleigh wing starts gaining in intensity (see Figure 6). Both in the spectrum of liquid and in the spectrum of matrix isolated THF, there is a single weak and broad line at  $283 \text{ cm}^{-1}$ , but in the spectrum of polycrystalline THF at 10 K, there are two medium weak bands, appearing at  $245$  and  $299 \text{ cm}^{-1}$  (Figure 8), in accordance with the work of Aleksanyan and Antipov [19] who observed them at  $249$  and  $303 \text{ cm}^{-1}$  at 20 K. The assignments provided by Cadioli et al. [20], which we verified by repeating the calculation of normal modes of twisted THF using Gaussian09 [26] at the b3lyp/6-31++G(d,p) level of theory, are shown in Table 1. Previous studies on the structure of the free THF molecule claim that either the  $C_s$  (envelope) [5,10] or the  $C_2$  (twisted) form is the most stable conformation [4,11,20]. The matrix isolation technique enables one to observe THF vibrational transitions in the environment more closely resembling that of a gas than that of a liquid, providing better resolution of the observed bands. In particular, while

calculation predicts two bands at 581 and 672  $\text{cm}^{-1}$  for  $C_2$  conformer, for the  $C_s$  conformer, the corresponding modes are predicted at 645 and 651  $\text{cm}^{-1}$ . The observed bands in the Raman spectrum of matrix isolated THF are at 577 and 662  $\text{cm}^{-1}$  (Table 1, Figure 6). Stocka et al. presented FTIR matrix isolated spectra of THF in the 600–3025  $\text{cm}^{-1}$  interval, and did not report any bands below 600  $\text{cm}^{-1}$  [22]. Instead, they followed the behavior of the 1073.1 and 898.9  $\text{cm}^{-1}$  bands on annealing, and concluded that both conformers are present in their matrix. Comparing the Raman spectra of matrix isolated THF with those of crystals (Figures 2–4), one finds a close resemblance of band positions and intensities, confirming our conclusion that only  $C_2$  is present in the matrix.

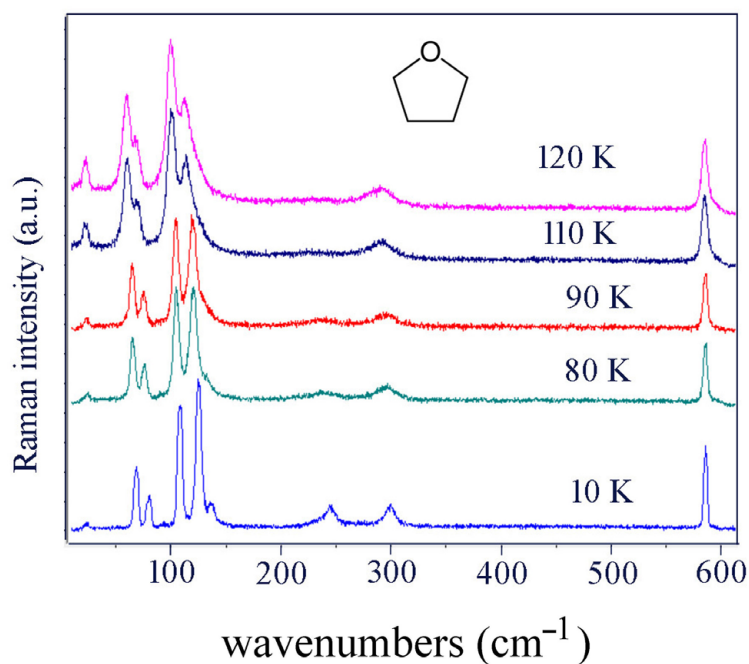


**Figure 8.** Temperature dependence of low-frequency Raman spectra of polycrystalline THF obtained at 120 K, 110 K, 90 K, 80 K and 10 K from 10–600  $\text{cm}^{-1}$ .

In the majority of organic compounds, vibrational bands observed in liquid usually split into several new bands, reflecting the strength of the intermolecular interactions experienced in solid. The difference in wavenumbers observed between new split bands is called crystal splitting, and can range from a few  $\text{cm}^{-1}$  to several tens of wavenumbers, depending on the type of molecular motion from which the band originates. In tetrahydrofuran crystals, Raman bands at 586 and 667  $\text{cm}^{-1}$  are narrow compared to 244 and 299  $\text{cm}^{-1}$  bands (Figure 8). While the 586  $\text{cm}^{-1}$  band corresponds to C-O-C bending coupled to  $\text{CH}_2$  rocking, the 667  $\text{cm}^{-1}$  is predominantly C-O-C bending vibration. No crystal splitting  $A_g/B_g$  is observed for these two bands in crystal; therefore, we do not think it likely that 245 and 299  $\text{cm}^{-1}$  bands are the  $A_g$  and  $B_g$  components of the radial mode observed at 283  $\text{cm}^{-1}$  in liquid and in the matrix. The normal mode of  $C_2$  THF having the lowest wavenumber is calculated to lie at 42  $\text{cm}^{-1}$ , while the following higher mode (referred to as the “radial” mode [12]) is at 251  $\text{cm}^{-1}$ . While the value obtained for the radial mode is closer to the 299  $\text{cm}^{-1}$  band observed in crystal (Figure 6), the band at 244  $\text{cm}^{-1}$ , which we assign to the quasi pseudorotational motion of THF in solid, is at much higher wavenumbers than calculated in the harmonic approximation for the twisted conformer in the free state.

Temperature dynamics of large amplitude motions can provide insights into molecular dynamics. For example, the internal rotation of methyl group in toluene and nitromethane was studied in detail by Cavagnat et al. [29]. The  $0A \rightarrow 1A$  and  $0E \rightarrow 1E$  transitions of internal rotation in  $\text{CH}_3\text{NO}_2$  that are observed in low-temperature Raman spectra show a weakening of intensity on heating, and merge into a single band at 50 K [29]. Another

small carbon ring compound, cyclobutane, has two solid phases: a plastic crystalline phase I just below the melting point, which occurs at 182 K, and crystal phase II, into which phase I transforms below 145 K [30]. Durig et al. recorded low-temperature Raman spectra of cyclobutane, and discovered that the puckering mode, which is observed as a strong band at  $257\text{ cm}^{-1}$  at 10 K, gradually loses its intensity and practically vanishes in the vicinity of transition into orientationally disordered phase I [31]. The same behavior is observed for the  $244\text{ cm}^{-1}$  tetrahydrofuran band (Figure 6), confirming the work of Aleksanyan and Antipov [19].

Small globular molecules tend to form plastic crystals, structures in which molecules have their centres of mass ordered on lattice points, but having orientational disorder to a certain degree [32]. Often, the fast-cooling of a plastically crystalline state produces a glassy crystal, which has its positional order preserved but orientational order frozen. Angell et al. proposed a guideline by which one can estimate whether a compound is prone to form a glassy crystal: if the ratio of the temperature of the boiling point  $T_b$  to temperature  $T_m$  of melting  $T_b/T_m$  is greater than 2, a compound may form a glassy crystal [33]. For tetrahydrofuran,  $T_b$  is 339 K [34], and the melting point as determined by Lebedev et al. is  $T_m = (164.9 \pm 0.2)\text{ K}$ , which gives us  $T_b/T_m$  of 2.055 [35]. One may thus question the possibility of the existence of a glassy state in THF—such a type was predicted by the molecular dynamics simulation method employed by Rong-Ri et al. [36], but ruled out after several attempts to achieve a vitrification in THF proved unsuccessful [35]. Considering that such a phase was found by Raman spectroscopy to exist in nitromethane in a very narrow temperature interval [37] and was not detected by the classical measurement of heat capacity [38], there is a possibility that tetrahydrofuran possesses such a phase as well.

## 5. Conclusions

Low-temperature Raman spectroscopy was applied to study the dynamics of tetrahydrofuran in the polycrystalline phase, and as a matrix isolated compound in air. The Raman spectrum of tetrahydrofuran isolated in air matrix was recorded for the first time, showing a better resolution of bands than is found in liquid. The width of bands observed in the spectrum of THF in air matrix, together with the observed low-frequency  $283\text{ cm}^{-1}$  band, suggests that THF molecules undergo free pseudorotational motion, which is hindered in crystal. The temperature dependence of the  $244\text{ cm}^{-1}$  band observed at 10 K in the spectrum of crystalline THF shows a progressive diminishing of its intensity towards melting point. This band was assigned as the hindered pseudorotational mode of the  $C_2$  conformer present in the crystal.

**Funding:** This work was partially supported by Centre of Excellence for Advanced Materials and Sensors, a project co-financed by the Croatian government and the European Union through the European regional development fund e The Competitiveness and Cohesion Operational Programme (KK.01.1.1.01). Calculations using Gaussian09 were performed at University of Zagreb Computing Centre SRCE.

**Data Availability Statement:** The original contributions presented in the study are included in the article, further inquiries can be directed to the corresponding author.

**Conflicts of Interest:** The author declares no conflict of interests.

## References

1. Grdadolnik, J.; Mohacek-Grosev, V.; Baldwin, R.L.; Avbelj, F. Populations of the three major backbone conformations in 19 amino acid dipeptides. *Proc. Natl. Acad. Sci. USA* **2011**, *108*, 1794–1798. [[CrossRef](#)] [[PubMed](#)]
2. Angyal, S.J. The Composition of Reducing Sugars in Solution. *Adv. Carboh. Chem. Biochem.* **1984**, *42*, 15–68. [[CrossRef](#)]
3. Arukawa, Y.; Komatsu, K.; Feng, J.; Zhu, C.; Tsuji, H. Distinct twist-bend nematic phase behaviors associated with the ester-linked liquid crystal dimers. *Mater. Adv.* **2021**, *2*, 261–272. [[CrossRef](#)]
4. Man Park, S.; Ho Kwon, S. Deciphering the conformational preference and ionization dynamics of tetrahydrofuran: Insights from advanced spectroscopic techniques. *J. Chem. Phys.* **2024**, *160*, 114308. [[CrossRef](#)] [[PubMed](#)]
5. Boese, A.D.; Boese, R. Tetrahydrothiophene and Tetrahydrofuran, Computational and X-ray Studies in the Crystalline Phase. *Cryst. Growth Des.* **2015**, *15*, 1073–1081. [[CrossRef](#)]

6. Bowron, D.T.; Finney, J.L.; Soper, A.K. The structure of liquid tetrahydrofuran. *J. Am. Chem. Soc.* **2006**, *128*, 5119–5126. [[CrossRef](#)] [[PubMed](#)]
7. Lee, H.; Lee, J.-W.; Kim, D.Y.; Park, J.; Seo, Y.-T.; Zeng, H.; Moudrakovski, I.L.; Ratcliffe, C.I.; Ripmeester, J.A. Tuning clathrate hydrates for hydrogen storage. *Nature* **2005**, *434*, 743–746. [[CrossRef](#)] [[PubMed](#)]
8. Ford, T.A. The evolution of the structural, vibrational and electronic properties of the cyclic ethers—On ring size. An ab initio study. *J. Mol. Struct.* **2014**, *1073*, 125–133. [[CrossRef](#)]
9. Yang, T.; Su, G.; Ning, C.; Deng, J.; Wang, F.; Zhang, S.; Ren, X.; Huang, Y. New Diagnostic of the Most Populated Conformer of Tetrahydrofuran in the Gas Phase. *J. Phys. Chem A* **2007**, *111*, 4927–4933. [[CrossRef](#)]
10. Rayon, V.M.; Sordo, J.A. Pseudorotation motion in tetrahydrofuran: An ab initio study. *J. Chem. Phys.* **2005**, *122*, 204303. [[CrossRef](#)]
11. Cremer, D.; Pople, J. Molecular orbital theory of the electronic structure of organic compounds. XXIII. Pseudorotation in saturated five-membered ring compounds. *J. Amer. Chem. Soc.* **1975**, *97*, 1358–1367. [[CrossRef](#)]
12. Sont, W.N.; Wieser, H. The radial transtion in tetrahydrofuran. *J. Raman Spectrosc.* **1981**, *11*, 334–338. [[CrossRef](#)]
13. Greenhouse, J.A.; Strauss, H.L. Spectroscopic Evidence for Pseudorotation. II. The Far-Infrared Spectra of Tetrahydrofuran and 1,3-Dioxolane. *J. Chem. Phys.* **1969**, *50*, 124–134. [[CrossRef](#)]
14. Engerholm, G.G.; Luntz, A.C.; Gwinn, W.D.; Harris, D.O. Ring Puckering in Five-Membered Rings. II. The Microwave Spectrum, Dipole Moment, and Barrier to Pseudorotation in Tetrahydrofuran. *J. Chem. Phys.* **1969**, *50*, 2446–2457. [[CrossRef](#)]
15. Mamleev, A.H.; Gunderova, L.N.; Galeev, R.V. Microwave Spectrum and Hindered Pseudorotation of Tetrahydrofuran. *J. Struct. Chem.* **2001**, *42*, 365–370. [[CrossRef](#)]
16. Melnik, D.G.; Gopalakrishnan, S.; Miller, T.A.; de Lucia, F.C. The absorption spectroscopy of the lowest pseudorotational states of tetrahydrofuran. *J. Chem. Phys.* **2003**, *118*, 3589–3599. [[CrossRef](#)]
17. Luger, P.; Buschmann, J. Twist conformation of Tetrahydrofuran in the Crystal. *Angew. Chem. Int. Ed. Engl.* **1983**, *22*, 410. [[CrossRef](#)]
18. David, W.I.F.; Ibberson, R.M. A reinvestigation of the structure of tetrahydrofuran by high-resolution neutron powder diffraction. *Acta Cryst. C* **1992**, *48*, 301–303. [[CrossRef](#)]
19. Aleksanyan, V.T.; Antipov, B.G. On the intramolecular dynamics of five-membered ring compounds in solid state. In *Raman Spectroscopy Linear and Nonlinear*; Lascombe, J., Huong, P., Eds.; John Wiley & Sons: New York, NY, USA, 1982; pp. 605–606.
20. Cadioli, B.; Gallinella, E.; Coulombeau, C.; Jobic, H.; Berthier, G. Geometric Structure and Vibrational Spectrum of Tetrahydrofuran. *J. Phys. Chem.* **1993**, *97*, 7844–7856. [[CrossRef](#)]
21. Gallinella, E.; Cadioli, B.; Flament, J.P.; Berthier, G. A scaled force field for tetrahydrofuran and its isotopomers from quantum mechanical calculations and infrared and Raman spectra. *J. Mol. Struct.* **1994**, *315*, 137–148. [[CrossRef](#)]
22. Stocka, J.; Čeponkus, J.; Šablinskas, V.; Rodziejewicz, P. Conformational diversity of the THF molecule in N<sub>2</sub> matrix by means of FTIR matrix isolation experiment and Car-Parrinello molecular dynamics simulations. *Spectrochim. Acta A Mol. Biomol. Spectrosc.* **2020**, *238*, 118425. [[CrossRef](#)] [[PubMed](#)]
23. Mohaček-Grošev, V.; Furić, K.; Vujnović, V. Raman study of water deposited in solid argon matrix. *Spectrochim. Acta A Mol. Biomol. Spectrosc.* **2022**, *269*, 120770. [[CrossRef](#)]
24. Furić, K.; Volovšek, V. Water ice at low temperatures and pressures: New Raman results. *J. Mol. Struct.* **2010**, *976*, 174–180. [[CrossRef](#)]
25. Available online: <https://webbook.nist.gov/cgi/cbook.cgi?ID=C109999&Mask=4&Type=ANTOINE&Plot=on> (accessed on 19 April 2024).
26. Frisch, M.J.; Trucks, G.W.; Schlegel, H.B.; Scuseria, G.E.; Robb, M.A.; Cheeseman, J.R.; Scalmani, G.; Barone, V.; Petersson, G.A.; Nakatsuji, H.; et al. (Eds.) *Gaussian 09, Revision A.02*; Gaussian, Inc.: Wallingford, CT, USA, 2016.
27. Berenblut, B.J.; Dawson, P.; Wilkinson, G.R. The Raman spectrum of gypsum. *Spectrochim. Acta* **1971**, *27A*, 1849–1863. [[CrossRef](#)]
28. Macrae, C.F.; Bruno, I.J.; Chisholm, J.A.; Edgington, P.R.; McCabe, P.; Pidcock, E.; Rodriguez-Monge, L.; Taylor, R.; van de Streek, J.; Wood, P.A. Mercury CSD 2.0—New Features for the Visualization and Investigation of Crystal Structures. *J. Appl. Cryst.* **2008**, *41*, 466–470. [[CrossRef](#)]
29. Cavagnat, D.; Lascombe, J.; Lassegues, J.C.; Horsewill, A.J.; Heidemann, A.; Suck, J.B. Neutron and Raman scattering studies of the methyl dynamics in solid toluene and nitromethane. *J. De Phys.* **1984**, *45*, 97–105. [[CrossRef](#)]
30. Stein, A.; Lehmann, C.W.; Luger, P. Crystal Structure of Cyclobutane at 117 K. *J. Am. Chem. Soc.* **1992**, *114*, 7684–7687. [[CrossRef](#)]
31. Durig, J.R.; Sullivan, J.F.; Durig, D.T. Low-frequency vibrational spectra of molecular crystals. XXII: Cyclobutane-d<sub>0</sub> and cyclobutane-d<sub>8</sub>. *Mol. Cryst. Liq. Cryst.* **1979**, *54*, 51–58. [[CrossRef](#)]
32. Sherwood, J.N. (Ed.) *The Plastically Crystalline State, Orientationally-Disordered Crystals*; John Wiley & Sons: Hoboken, NJ, USA, 1979.
33. Angell, C.A.; Busse, L.E.; Cooper, E.I.; Kadiyale, R.K.; Dworkin, A.; Ghelfenstein, M.; Szwarc, H.; Vassal, A. Glasses and glassy crystals from molecular and molecular ionic systems. *J. Chim. Phys. Paris* **1985**, *82*, 267–274. [[CrossRef](#)]
34. NIH National Library of Medicine. Available online: <https://pubchem.ncbi.nlm.nih.gov/compound/Tetrahydrofuran> (accessed on 1 May 2024).
35. Lebedev, B.V.; Rabinovich, I.B.; Milov, I.V.; Lityagor, V.Y. Thermodynamic properties of tetrahydrofuran from 8 K to 322 K. *J. Chem. Thermodyn.* **1978**, *10*, 321–329. [[CrossRef](#)]

36. Rong-Ri, T.; Xin, S.; Lin, H.; Feng-Shon, Z. Liquid glass transition of tetrahydrofuran and 2-methyltetrahydrofuran. *Chin. Phys. B* **2012**, *21*, 086402. [[CrossRef](#)]
37. Mohaček Grošev, V.; Stelzer, F.; Jocham, D. Internal rotation dynamics of nitromethane at low temperatures. *J. Mol. Struct.* **1999**, *476*, 181–189. [[CrossRef](#)]
38. Cavagnat, D.; Brom, H.; Nugteren, P.R. Methyl internal rotation in partially deuterated molecular solids: The NO<sub>2</sub>CHD<sub>2</sub> and NO<sub>2</sub>CH<sub>2</sub>D systems. *J. Chem. Phys.* **1987**, *87*, 801–808. [[CrossRef](#)]

**Disclaimer/Publisher's Note:** The statements, opinions and data contained in all publications are solely those of the individual author(s) and contributor(s) and not of MDPI and/or the editor(s). MDPI and/or the editor(s) disclaim responsibility for any injury to people or property resulting from any ideas, methods, instructions or products referred to in the content.